



Published in final edited form as:

*Cancer Discov.* 2013 November ; 3(11): 1245–1253. doi:10.1158/2159-8290.CD-13-0172.

## Androgen receptor signaling regulates DNA repair in prostate cancers

William R. Polkinghorn<sup>1,2</sup>, Joel S. Parker<sup>9,10</sup>, Man X. Lee<sup>1</sup>, Elizabeth M. Kass<sup>3</sup>, Daniel E. Spratt<sup>1</sup>, Phillip J. Iaquinta<sup>1</sup>, Vivek K. Arora<sup>1,4</sup>, Wei-Feng Yen<sup>5</sup>, Ling Cai<sup>1</sup>, Deyou Zheng<sup>11</sup>, Brett S. Carver<sup>1,6</sup>, Yu Chen<sup>1,4</sup>, Philip A. Watson<sup>1</sup>, Neel P. Shah<sup>1</sup>, Sho Fujisawa<sup>7</sup>, Alexander G. Goglia<sup>2</sup>, Anuradha Gopalan<sup>7</sup>, Haley Hieronymus<sup>1</sup>, John Wongvipat<sup>1</sup>, Peter T. Scardino<sup>6</sup>, Michael J. Zelefsky<sup>1</sup>, Maria Jasin<sup>3</sup>, Jayanta Chaudhuri<sup>5</sup>, Simon N. Powell<sup>2</sup>, and Charles L. Sawyers<sup>1</sup>

<sup>1</sup>Memorial Sloan-Kettering Cancer Center, Human Oncology Pathogenesis Program

<sup>2</sup>Memorial Sloan-Kettering Cancer Center, Department of Radiation Oncology

<sup>3</sup>Memorial Sloan-Kettering Cancer Center, Developmental Biology Program

<sup>4</sup>Memorial Sloan-Kettering Cancer Center, Department of Medicine

<sup>5</sup>Memorial Sloan-Kettering Cancer Center, Immunology Program

<sup>6</sup>Memorial Sloan-Kettering Cancer Center, Department of Surgery

<sup>7</sup>Memorial Sloan-Kettering Cancer Center, Molecular Cytology Core Facility

<sup>8</sup>Memorial Sloan-Kettering Cancer Center, Department of Pathology, New York, New York

<sup>9</sup>University of North Carolina, Department of Genetics, Chapel Hill, North Carolina

<sup>10</sup>University of North Carolina, Lineberger Comprehensive Cancer Center, Chapel Hill, North Carolina

<sup>11</sup>Albert Einstein College of Medicine, Department of Genetics, New York, New York

### Abstract

We demonstrate that the androgen receptor (AR) regulates a transcriptional program of DNA repair genes that promotes prostate cancer radioresistance, providing a potential mechanism by which androgen deprivation therapy (ADT) synergizes with ionizing radiation (IR). Using a model of castration-resistant prostate cancer, we show that second-generation antiandrogen therapy results in downregulation of DNA repair genes. Next, we demonstrate that primary prostate cancers display a significant spectrum of AR transcriptional output which correlates with expression of a set of DNA repair genes. Employing RNA-seq and ChIP-seq, we define which of these DNA repair genes are both induced by androgen and represent direct AR targets. We establish that prostate cancer cells treated with IR plus androgen demonstrate enhanced DNA repair and decreased DNA damage and furthermore that antiandrogen treatment causes increased DNA damage and decreased clonogenic survival. Finally, we demonstrate that antiandrogen treatment results in decreased classical non-homologous end joining.

---

Corresponding Author: Charles L. Sawyers, M.D., Investigator, Howard Hughes Medical Institute, Chairman, Human Oncology and Pathogenesis Program, Memorial Sloan-Kettering Cancer Center, New York, NY, 10065, Phone: (646) 888-2138; Fax: (646) 888-3407, sawyerc@mskcc.org.

Conflict of interest statement: CLS and JW are co-inventors of ARN-509.

## Introduction

Multiple clinical trials comparing radiotherapy (RT) plus androgen deprivation therapy (ADT) versus RT alone for high-risk prostate cancer, and more recently intermediate-risk, show significant improvement in disease-free and overall survival with the addition of ADT (1, 2). Furthermore, post-treatment biopsy series demonstrate improved local control when ADT is added to RT (3). In light of these and other studies, combining ADT with RT for high-risk prostate cancer has been the standard of care for nearly twenty years, yet the mechanism by which ADT improves patient outcomes remains unknown. Furthermore, it is unknown whether ADT benefits a subset of patients substantially or all patients with prostate cancer to a smaller degree.

Given the compelling body of clinical evidence, many have sought to elucidate how inhibiting the androgen receptor (AR) potentiates ionizing radiation (IR). Using *in vitro* and *in vivo* models, the addition of ADT to IR has been shown to increase prostate cancer cell death (4). A number of mechanisms have been explored to explain the increase in cell death when ADT is combined with IR, including decreased tumor cell hypoxia (5), decreased DNA repair (6), or simply decreased AR-mediated cell growth independent of direct synergy (7). Surprising light has recently been shed on additional inter-relationships between AR and DNA repair, including a role for AR in mediating prostate-cancer specific translocations following high-dose IR (8) and the discovery that the DNA repair protein, PARP1, is an important co-factor for AR transcriptional activity (9).

Defining the mechanism by which ADT increases prostate cancer radioresponse has never been more clinically relevant given the recently demonstrated success of second-generation anti-androgens in the treatment of castration-resistant patients (10, 11). Given the clinical potential of deploying these new agents as part of radiotherapy for primary disease coupled with the ability now to leverage prostate cancer genomics data to help define genetic mechanisms in a less biased way, it is critical to re-examine the basic biologic question of how AR signaling promotes prostate cancer radioresistance.

## Results

We began with an unbiased query of how gene expression is perturbed when a clinically validated xenograft model of castration-resistant prostate cancer, LNCaP-AR, is treated with the second-generation anti-androgen, ARN-509 (12, 13). After four days of treatment with ARN-509, transcriptome analysis was performed by Illumina HT12 expression array. Standard gene set enrichment analysis (GSEA) was performed, and, to our surprise, three out of the top ten gene sets that were enriched in the control versus ARN-509-treated groups represented DNA repair gene sets; in total, 6 DNA repair gene sets comprised the top 50 enriched gene sets (Fig. 1A, Supplementary Table S1).

Given the unexpected result of ADT decreasing DNA repair gene expression in the castration-resistant model, we next sought to determine whether there was an association of AR transcriptional output with DNA repair genes in primary, castration-sensitive human prostate tumors (14). This set of primary prostate cancer tumors represents the appropriate group to analyze since this is the disease state treated with ADT and RT. First, we determined the variance of canonical AR transcriptional output, using a well-known signature derived by Hieronymus *et al.* (14, 15) across primary human prostate cancer tumors. Again, to our surprise, we observed a large spectrum of canonical AR output (Fig. 1B). Given this variance of AR output across primary prostate cancer tumors, we next asked whether there was a correlation between a composite score of canonical AR output, as previously calculated (16), and a composite score of the enriched DNA repair genes from

the previous xenograft experiment. Upon this analysis, we indeed found a significant correlation ( $p < 0.001$ ) between canonical AR output and the enriched DNA repair genes (Fig. 1C). Next, in order to define the most robust signature of AR-associated DNA repair genes without limiting ourselves to the enriched genes from the initial xenograft experiment, we more broadly asked which of the DNA repair genes in all of the six combined DNA repair gene sets (294 genes) were most associated with canonical AR output in the primary human prostate cancer data set (Fig. 1D, Supplementary Table S2). Filtering for an association with canonical AR output ( $p < 0.01$  and  $r > 0$ ), we defined an “AR-associated DNA repair gene” signature of 144 DNA repair genes that were significantly associated with canonical AR output.

Given the association of canonical AR output with DNA repair gene expression in primary prostate cancers, we next sought to determine using an *in vitro* model which, if any, of these DNA repair genes are transcriptionally regulated by androgen. We selected the most widely studied prostate cancer cell line, LNCaP, to model primary prostate cancer. After treating LNCaP prostate cancer cell line with synthetic androgen (R1881) for two days and comparing to vehicle-treated (DMSO) cells, we measured gene expression level changes by RNA-seq and identified AR target genes by AR ChIP-seq. We first confirmed that our newly defined, 144-gene AR-associated DNA repair gene signature was in fact enriched by GSEA in the androgen-treated samples, in addition to other well-known AR signatures such as Nelson *et al.* (Fig. 2A) (17). Of the 144 genes that comprise the AR-associated DNA repair signature, we next identified those genes whose expression was increased by androgen and which contained AR binding sites (Fig. 2B). 32 genes were both induced by androgen and exhibited AR peaks in their enhancers (32) or promoter (1), suggesting that these represented *bona fide* AR target genes (Fig. 2B and 2C, Supplementary Fig. 2). Motif analysis of the AR binding peaks of these 32 genes revealed the classic consensus AR-binding site (Fig. 2D).

We next sought to determine whether the reduction in DNA repair gene expression observed with androgen deprivation was associated with (1) reduced DNA repair and (2) increased DNA damage. Using the same *in vitro* LNCaP model, we exposed prostate cancer cells, pretreated for two days with either synthetic androgen (1 nM R1881) or mock (DMSO), to 2 Gy of IR and gamma-H2AX foci were quantified. Comparing the gamma-H2AX foci in the two conditions, we found that in androgen-depleted conditions the foci peaked later and higher and resolved more slowly, consistent with decreased repair (Fig. 3A). Since gamma-H2AX foci represent a surrogate, indirect marker of unrepaired breaks, we next sought to measure DNA damage itself. To do so, we employed the neutral Comet assay that directly measures double-strand DNA breaks. The findings of the Comet assay under the same conditions recapitulated the results obtained analyzing gamma-H2AX foci (Fig. 3B). Of note, at baseline after 48 hours of pretreatment (time 0), mock-treated cells demonstrated increased gamma-H2AX foci and increased DNA damage by Comet assay. However, after normalizing the findings from both assays to each condition's respective time 0, the post-IR findings of relative decreased repair and increased damage persisted (Supplementary Fig. S1). Given the surprising result that even in the absence of IR that androgen deprivation alone exhibited increased DNA damage compared to androgen-treated cells, we next asked whether treatment with ARN-509 would also increase DNA damage relative to control. After 48 hours of ARN-509 (1  $\mu$ M) treatment versus mock (DMSO), we found increased DNA damage in LNCaP cells, a finding we then demonstrated in two additional cell lines, LNCaP-AR and VCaP (Fig. 3C).

Given these findings, we next asked whether antiandrogen-treated cells compared to mock-treated cells exhibited decreased cell viability following IR. To do so, we employed the classic clonogenic assay using the LNCaP cell line and demonstrated that treatment with

ARN-509 (1  $\mu$ M) compared to mock (DMSO) resulted in decreased cell survival (Fig. 3D). To further address the possibility that the enhanced radiosensitivity observed with androgen deprivation therapy (ADT) is not due to partial synchronization of rapidly dividing cells into more radiosensitive phases of the cell cycle, we measured the percentage of LNCaP cells in G1, S and G2/M in androgen-deprived cells (DMSO) compared to a range of doses of R1881 in charcoal-stripped serum, each for 48 hours. The percentage of cells across the phases of the cell cycle did not change, yet increasing concentrations of androgen resulted in increased cell growth except for the highest concentration (10 nM) (Supplementary Fig. S2). We repeated this analysis for LNCaP cells treated with ARN-509 versus control for 48 hours, and again found no meaningful change in cell cycle distribution (Supplementary Fig. S3).

Given these findings that AR transcriptionally regulates a network of DNA repair genes and that antiandrogen treatment increases DNA damage and radiosensitizes cells, we next sought to determine which of DNA repair pathways are functionally abrogated by ARN-509 (Fig. 4A). Since the DNA double-strand breaks (DSBs) induced by IR are thought to be repaired by classical nonhomologous end-joining (C-NHEJ) and homologous recombination (HR), we focused upon these repair pathways.

In order to assess the effects of antiandrogen treatment on C-NHEJ, we employed the transient V(D)J recombination assay as previously described (Fig. 4B) (18, 19). The V(D)J recombination substrate along with RAG1 and RAG2 expression vectors were transfected into LNCaP cells that had been pretreated for 48 hours with either mock (DMSO) or ARN-509 (1  $\mu$ M). In this assay, rescued substrate plasmids that fail to undergo C-NHEJ-dependent recombination only express the ampicillin (Amp) resistant gene, while those that successfully undergo recombination express both Amp and chloramphenicol (Cam) resistant genes. Therefore, after transforming bacteria with the rescued substrate, a recombination frequency can be calculated by the ratio of colonies grown on the Amp + Cam plates compared to the Amp plates. Compared to control treatment, ARN-509-treated cells demonstrated significantly decreased C-NHEJ-mediated recombination (>60%), comparable to that seen with stable Lig4 knockdown (Fig. 4C, Supplementary Fig. S4). Next, to assess the effects of antiandrogen treatment on HR, we utilized the transient DR-GFP assay, a widely used repair reporter assay for studying HR (Fig. 4D) (20). DR-GFP contains direct repeats of two defective GFP genes with the upstream repeat containing a recognition site for the I-SceI endonuclease. A double-strand break induced by I-SceI followed by gene conversion with the downstream copy results in a functional GFP gene, and GFP<sup>+</sup> cells can be scored by flow cytometry. Using this assay, no significant difference in HR was observed between the treated and control cells, in contrast to the 2.8 fold reduction in HR observed with expression of BRC3, a peptide known to interfere with HR (Fig. 4E) (21).

## Discussion

Androgens, acting through AR, regulate a complex transcriptional program for both prostate cancer growth and differentiation, with recent data demonstrating unique sets of AR target genes in castration-sensitive versus castration-resistant tumors (22). In this study, we discover a network of DNA repair genes that comprises part of the complex AR-regulated transcriptome. Our data establish that AR signaling increases the expression of DNA repair genes and, in parallel, promotes prostate cancer radioresistance by accelerating repair of IR-induced DNA damage. Collectively, these data provide strong mechanistic rationale for the observed synergy between ADT and RT.

Clinical trials of ADT plus RT have been unable to answer the question of whether ADT benefits all patients modestly or a subset to a greater degree. The surprising spectrum of AR

output that we observe in primary prostate cancer tumors suggests that ADT may preferentially benefit those patients with high AR transcriptional output and, consequently, high expression of DNA repair genes. Therefore, in a similar manner that breast cancer patients are selected for anti-estrogen therapy by a molecular determinant of response (ER/PR status), perhaps it is possible to select prostate cancer patients who will receive ADT along with RT (as opposed to RT alone) based upon a tumor's AR output. This hypothesis could be tested using pathologic specimens from one of the landmark clinical trials comparing ADT and RT to RT alone.

The discovery that AR activity, among its other known biologic effects, also regulates DNA repair could have implications beyond the question of how ADT synergizes with RT. First, the finding that C-NHEJ can be dynamically modulated via inhibition of a nuclear hormone receptor/transcription factor represents a new kind of mechanism by which to abrogate this important pathway. Second, it remains to be determined whether the other identified AR-regulated DNA repair genes play a functional role in their respective pathways (e.g. mismatch repair, base excision repair, Fanconi pathway) when their expression levels are modulated by AR (Fig. 4A). Finally, recent genomic studies demonstrate that in comparison to primary tumors, one of the hallmarks of CRPC appears to be widespread genomic instability (14, 23). The possibility that the therapeutic intervention of ADT itself during the several-year period of castration-sensitivity may contribute to the genomic instability observed in castration-resistant tumors raises a number of important future directions for investigation.

## Methods

### LNCaP/AR xenografts

LNCaP/AR xenografts were established in castrate mice as described previously and, once established, were treated for four days with either 10 mg/kg ARN-509 (San Diego, CA) plus vehicle (1% carboxymethyl cellulose, 0.1% Tween-80, 5% DMSO) or vehicle alone (12). RNA was isolated per standard protocol and expression profiling performed using Illumina HT-12 array (Arora *et al.* in preparation). Gene set enrichment analysis (24) was used to test for pathway level differential expression. Discovery analysis of the xenograft transcriptomes utilized all gene sets listed in both the curated (c2) and gene ontology (c5) of the Broad Institute's Molecular Signature Databases (MSigDB).

### Determining association between canonical AR output DNA repair genes

Canonical AR output was quantified using an unweighted summed score of the n-gene AR-responsive gene signature defined in Hieronymus *et al.* (15). The initial set of DNA repair candidates was taken as the union of the 6 DNA repair associated signatures resulting from the xenograft experiment. The correlation between the AR signature and each candidate gene was calculated. Results were filtered to identify all DNA repair associated genes with significant (Pearson correlation,  $p < 0.01$ ) positive correlations. The resulting candidates were summarized to the within sample mean as a relative measure of the signature. Spearman correlation was used to test for significant relationship between the AR and DNA repair signatures.

### LNCaP RNA-Seq/ChIP-Seq

LNCaP cells were grown in described conditions in triplicate and RNA was isolated by Rneasy Mini Kit (Qiagen) with the additional steps of lysate homogenization using QIAshredder (Qiagen) and DNase digestion using RNase-Free DNase Set (Qiagen). Samples were prepared and libraries created using TruSeq RNA Sample Preparation Kit v2 (Illumina), which included a poly A selection step. Libraries were pooled at 2 nm



concentration and the samples were then subject to cBot cluster generation using TruSeq Rapid PE Cluster Kit (Illumina). The amplified libraries were sequenced using the TruSeq Rapid SBS Kit on the HiSeq 2500 (Illumina). mRNA-seq data were aligned with Mapssplice(25) and genes were quantified with RSEM.(26) Gene expression estimates were log transformed and upper quartile normalized. Differential expression was measured using unequal variance t-test to identify candidate genes. GSEA analysis of the cell line data was used to test if the 144 AR associated DNA repair genes were associated with 1881 treatment relative to DMSO. AR ChIP-Seq was performed according to Cai L *et al.* (in preparation).

### Cell irradiation

All described doses of IR was delivered using Cs-137 irradiator (Shepherd Mark, Model 68) at a dose rate of 184 cGy/min and at a turntable speed of 6 revolutions/minute.

### Gamma-H2AX assay

LNCaP cells were grown in described conditions for two days on CC2-coated, 4-chamber slides (Nunc Lab-Tek II, Thermo Scientific), approximately 20,000 cells per well in 500uL total volume, and following IR were washed and fixed with 4% PFA and 0.2% Triton X-100. Slides were blocked with 10% FBS and 0.5% Triton X-100, and the primary antibody (Gamma-H2AX, Millipore) incubated overnight at 4 degrees. Slides were then washed, incubated with secondary antibody (Alexa Fluor 488 Dye, Life Technologies) for one hour at room temperature, and stained for DAPI. Slides were scanned by confocal microscopy (LSM 5 LIVE) with a 20X/0.8NA objective and foci were counted by Metamorph image analysis software (Molecular Devices). For each time point, on average foci of 2,000 separate nuclei were counted.

### Neutral Comet assay

LNCaP, LNCaP-AR, and VCaP cells were grown in described conditions for two days and neutral Comet assay performed using CometAssay® Electrophoresis System (Trevigen) per assay protocol (27).

### Clonogenic assay

LNCaP cells were grown in 10cm tissue-culture treated polystyrene dishes (BD Falcon) in described conditions for two days prior to irradiation. Cells received either 0, 2, 5, or 10 Gy of IR, and were subsequently replated in respective conditions into 6-well, tissue-culture treated polystyrene plates (BD Falcon) in a series of 1/3 dilutions (24,000, 8,000, 2,667, 867, 289, and 96 cells per well) at each dose. Lethally irradiated HeLa feeder cells (400,000) were added to each well to promote colony formation. Plates were incubated for 14 days, then washed and fixed with methanol, and stained with 0.2% crystal violet (Sigma) in 10% formalin (Sigma). Plates were scanned by GelCount (Oxford Optronix), and colonies were counted using GelCount software. Clonogenic survival curves were generated as previously described.

### Western blot analysis

Whole cell lysates were prepared using 10% M-PER lysis buffer and clarified by centrifugation. Proteins were separated by 4–12% SDS-PAGE gel and transferred onto PVDF membranes (Invitrogen). After primary antibody incubation (LIG4, Abcam; GAPDH, Abcam) for one hour at room temperature, washings, and incubation with secondary antibodies, blots were developed with a chemiluminescence system (Pierce).

## Transient V(D)J recombination assay

The transient V(D)J recombination assay was performed as described according to Lieber and colleagues (18, 19). The V(D)J recombination substrate plasmid along with RAG1 and RAG2 expression vectors were transfected into LNCaP cells ( $2 \times 10^6$ ) pretreated for 48 hours with either mock (DMSO) or ARN-509 (1  $\mu$ M), or the same cell line infected with shNT or shLig4 lentiviral vectors (Sigma-Aldrich). Plasmids were retrieved 48 hours following transfection, and electrocompetent bacteria (Mega-X DH10B, Invitrogen) were then transformed with the rescued substrate plasmids and plated on both ampicillin (Amp) and ampicillin + chloramphenicol (Amp + Cam) plates. Bacteria were plated at 1:1000–5000 dilution for Amp plates and 1:10–50 dilution for Amp + Cam plates in order to grow colonies at numbers that could be quantified by manual counting. Substrate plasmids that failed to undergo recombination by C-NHEJ only expressed the ampicillin resistant gene (Amp<sup>r</sup>), while plasmids that underwent successful recombination expressed both Amp<sup>r</sup> and chloramphenicol (Cam<sup>r</sup>) resistant genes. Recombination efficiency was calculated by the ratio of the colonies grown on the Amp + Cam plates to the Amp plates.

## DR-GFP Assay

To measure DSB repair by HR,  $2 \times 10^6$  LNCaP cells were nucleofected with 0.7  $\mu$ g of DR-GFP plasmid and 2  $\mu$ g I-SceI expression vector (pCBASce) and 1.3  $\mu$ g empty vector (pCAGGS) or 3.3  $\mu$ g pCAGGS or for a positive control 2 $\mu$ g NZEGFP and 2 $\mu$ g pCAGGS (20). After transfection, cells were immediately plated in regular medium containing 1  $\mu$ M ARN-509 or control (DMSO). For BRC3 experiments,  $2 \times 10^6$  LNCaP cells were nucleofected with 0.7  $\mu$ g of DR-GFP plasmid, 2  $\mu$ g I-SceI expression vector (pCBASce) and 2  $\mu$ g of BRC3 expression plasmid or empty vector (pCAGGS) (21). Flow cytometry was performed 48 h after transfection to analyze GFP expression.

## Cell lines

LNCaP and VCaP cell lines used in this manuscript were purchased directly from ATCC (Manassas, VA) and cultured according to specifications. LNCaP-AR is an AR-overexpressing (wild type) cell line originally derived from parental LNCaP; the LNCaP-AR cell line was authenticated for AR overexpression by immunoblot.

## Supplementary Material

Refer to Web version on PubMed Central for supplementary material.

## Acknowledgments

Funding source: Prostate Cancer Foundation, Creativity Award (2011)

We thank M.R. Lieber (University of Southern California) for graciously providing us the plasmids for the transient V(D)J recombination assay. In addition, W.R. Polkinghorn wishes to thank T.G. Bivona for his encouragement and friendship and C.L. Sawyers for both the opportunity to pursue this important question and teaching him to become a scientist along the way.

## References

1. Bolla M, Gonzalez D, Warde P, Dubois JB, Mirimanoff RO, Storme G, et al. Improved survival in patients with locally advanced prostate cancer treated with radiotherapy and goserelin. *N Engl J Med.* 1997; 337:295–300. [PubMed: 9233866]
2. Jones CU, Hunt D, McGowan DG, Amin MB, Chetner MP, Bruner DW, et al. Radiotherapy and short-term androgen deprivation for localized prostate cancer. *N Engl J Med.* 2011; 365:107–18. [PubMed: 21751904]

3. Zelefsky MJ, Reuter VE, Fuks Z, Scardino P, Shippy A. Influence of local tumor control on distant metastases and cancer related mortality after external beam radiotherapy for prostate cancer. *J Urol*. 2008; 179:1368–73. discussion 73. [PubMed: 18289585]
4. Wo JY, Zietman AL. Why does androgen deprivation enhance the results of radiation therapy? *Urol Oncol*. 2008; 26:522–9. [PubMed: 18774467]
5. Jain RK, Safabakhsh N, Sckell A, Chen Y, Jiang P, Benjamin L, et al. Endothelial cell death, angiogenesis, and microvascular function after castration in an androgen-dependent tumor: role of vascular endothelial growth factor. *Proc Natl Acad Sci U S A*. 1998; 95:10820–5. [PubMed: 9724788]
6. Al-Ubaidi FL, Schultz N, Egevad L, Granfors T, Loseva O, Helleday T. Castration therapy results in decreased Ku70 levels in prostate cancer. *Clin Cancer Res*. 2013
7. Pollack A, Salem N, Ashoori F, Hachem P, Sangha M, von Eschenbach AC, et al. Lack of prostate cancer radiosensitization by androgen deprivation. *Int J Radiat Oncol Biol Phys*. 2001; 51:1002–7. [PubMed: 11704324]
8. Lin C, Yang L, Tanasa B, Hutt K, Ju BG, Ohgi K, et al. Nuclear receptor-induced chromosomal proximity and DNA breaks underlie specific translocations in cancer. *Cell*. 2009; 139:1069–83. [PubMed: 19962179]
9. Schiewer MJ, Goodwin JF, Han S, Brenner JC, Augello MA, Dean JL, et al. Dual roles of PARP-1 promote cancer growth and progression. *Cancer discovery*. 2012; 2:1134–49. [PubMed: 22993403]
10. Scher HI, Fizazi K, Saad F, Taplin ME, Sternberg CN, Miller K, et al. Increased survival with enzalutamide in prostate cancer after chemotherapy. *N Engl J Med*. 2012; 367:1187–97. [PubMed: 22894553]
11. de Bono JS, Logothetis CJ, Molina A, Fizazi K, North S, Chu L, et al. Abiraterone and increased survival in metastatic prostate cancer. *N Engl J Med*. 2011; 364:1995–2005. [PubMed: 21612468]
12. Tran C, Ouk S, Clegg NJ, Chen Y, Watson PA, Arora V, et al. Development of a second-generation antiandrogen for treatment of advanced prostate cancer. *Science*. 2009; 324:787–90. [PubMed: 19359544]
13. Clegg NJ, Wongvipat J, Joseph JD, Tran C, Ouk S, Dilhas A, et al. ARN-509: a novel antiandrogen for prostate cancer treatment. *Cancer Res*. 2012; 72:1494–503. [PubMed: 22266222]
14. Taylor BS, Schultz N, Hieronymus H, Gopalan A, Xiao Y, Carver BS, et al. Integrative genomic profiling of human prostate cancer. *Cancer Cell*. 2010; 18:11–22. [PubMed: 20579941]
15. Hieronymus H, Lamb J, Ross KN, Peng XP, Clement C, Rodina A, et al. Gene expression signature-based chemical genomic prediction identifies a novel class of HSP90 pathway modulators. *Cancer Cell*. 2006; 10:321–30. [PubMed: 17010675]
16. Carver BS, Chapinski C, Wongvipat J, Hieronymus H, Chen Y, Chandralapaty S, et al. Reciprocal feedback regulation of PI3K and androgen receptor signaling in PTEN-deficient prostate cancer. *Cancer Cell*. 2011; 19:575–86. [PubMed: 21575859]
17. Nelson PS, Clegg N, Arnold H, Ferguson C, Bonham M, White J, et al. The program of androgen-responsive genes in neoplastic prostate epithelium. *Proc Natl Acad Sci U S A*. 2002; 99:11890–5. [PubMed: 12185249]
18. Gauss GH, Lieber MR. Unequal signal and coding joint formation in human V(D)J recombination. *Molecular and cellular biology*. 1993; 13:3900–6. [PubMed: 8321197]
19. Gauss GH, Lieber MR. Mechanistic constraints on diversity in human V(D)J recombination. *Molecular and cellular biology*. 1996; 16:258–69. [PubMed: 8524303]
20. Pierce AJ, Johnson RD, Thompson LH, Jasin M. XRCC3 promotes homology-directed repair of DNA damage in mammalian cells. *Genes & development*. 1999; 13:2633–8. [PubMed: 10541549]
21. Stark JM, Pierce AJ, Oh J, Pastink A, Jasin M. Genetic steps of mammalian homologous repair with distinct mutagenic consequences. *Molecular and cellular biology*. 2004; 24:9305–16. [PubMed: 15485900]
22. Sharma NL, Massie CE, Ramos-Montoya A, Zecchini V, Scott HE, Lamb AD, et al. The androgen receptor induces a distinct transcriptional program in castration-resistant prostate cancer in man. *Cancer Cell*. 2013; 23:35–47. [PubMed: 23260764]



23. Grasso CS, Wu YM, Robinson DR, Cao X, Dhanasekaran SM, Khan AP, et al. The mutational landscape of lethal castration-resistant prostate cancer. *Nature*. 2012; 487:239–43. [PubMed: 22722839]
24. Subramanian A, Tamayo P, Mootha VK, Mukherjee S, Ebert BL, Gillette MA, et al. Gene set enrichment analysis: a knowledge-based approach for interpreting genome-wide expression profiles. *Proc Natl Acad Sci U S A*. 2005; 102:15545–50. [PubMed: 16199517]
25. Wang K, Singh D, Zeng Z, Coleman SJ, Huang Y, Savich GL, et al. MapSplice: accurate mapping of RNA-seq reads for splice junction discovery. *Nucleic Acids Res*. 2010; 38:e178. [PubMed: 20802226]
26. Li B, Dewey CN. RSEM: accurate transcript quantification from RNA-Seq data with or without a reference genome. *BMC bioinformatics*. 2011; 12:323. [PubMed: 21816040]
27. Chen WT, Alpert A, Leiter C, Gong F, Jackson SP, Miller KM. Systematic identification of functional residues in mammalian histone H2AX. *Molecular and cellular biology*. 2013; 33:111–26. [PubMed: 23109425]

**Statement of significance**

We demonstrate that the androgen receptor (AR) regulates a network of DNA repair genes, providing a potential mechanism by which androgen deprivation synergizes with radiotherapy for prostate cancer.

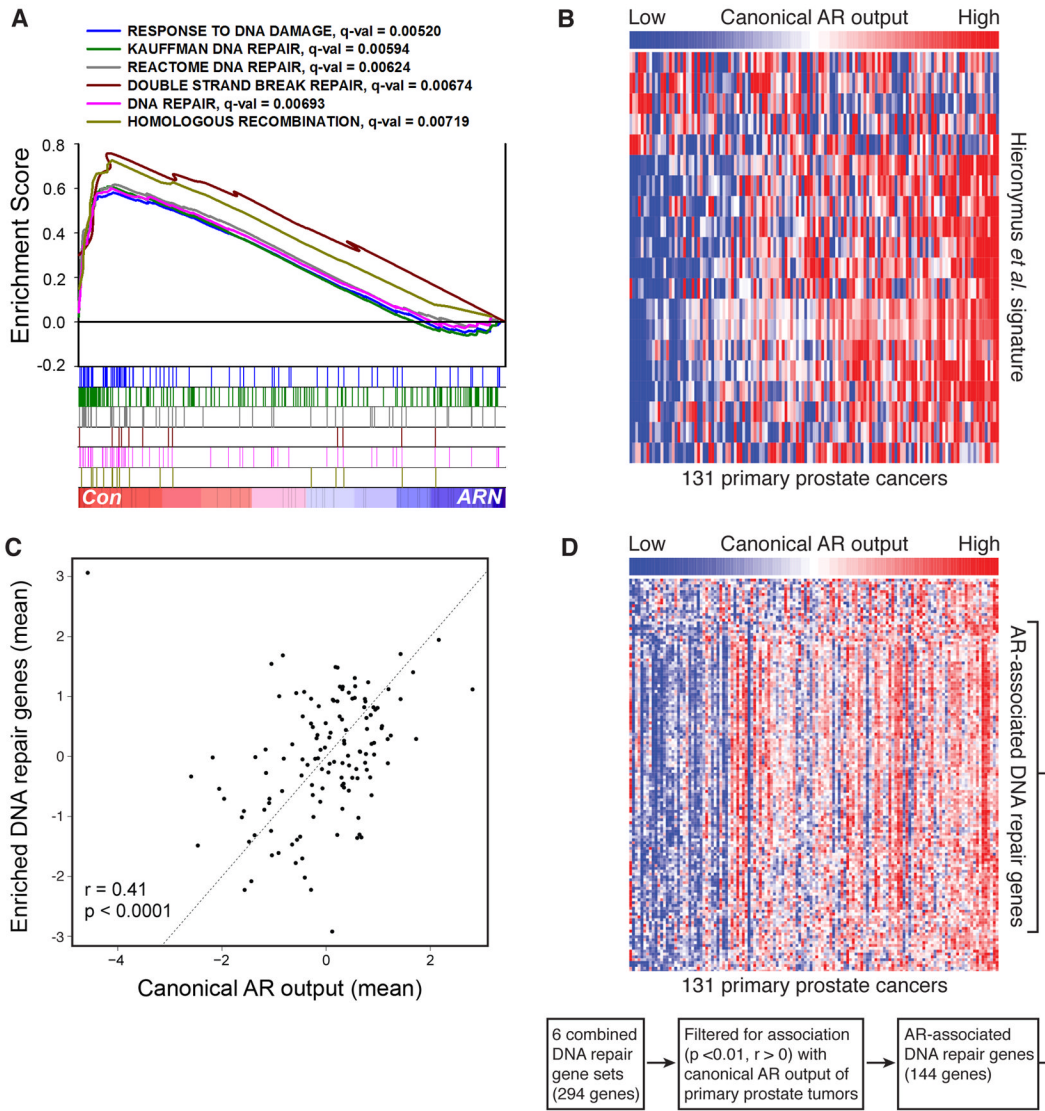


**Figure 1. AR transcriptional output is associated with expression of DNA repair genes**

**A.** Gene set enrichment analysis of second-generation anti-androgen (ARN-509) treatment of a castration-resistant xenograft model (LNCaP-AR). Xenografts were treated with 4 days of either control (red) or ARN-509 (blue). **B.** Heatmap demonstrating wide spectrum of AR transcriptional output (“canonical AR output”), calculated using Hieronimus *et al.* (18), across cohort of 131 primary prostate cancer tumors. **C.** Correlation between enriched DNA repair genes from the xenograft experiment (Fig. 1A) and canonical AR output in primary prostate cancer cohort. **D.** Union of top six enriched DNA repair gene sets from xenograft experiment filtered for an association with canonical AR output ( $p < 0.01$  and  $r > 0$ ) in same human cohort. Primary prostate tumors ranked from low to high canonical AR output, left to right, with corresponding heatmap of associated 144 DNA repair genes (“AR-associated DNA repair” signature).

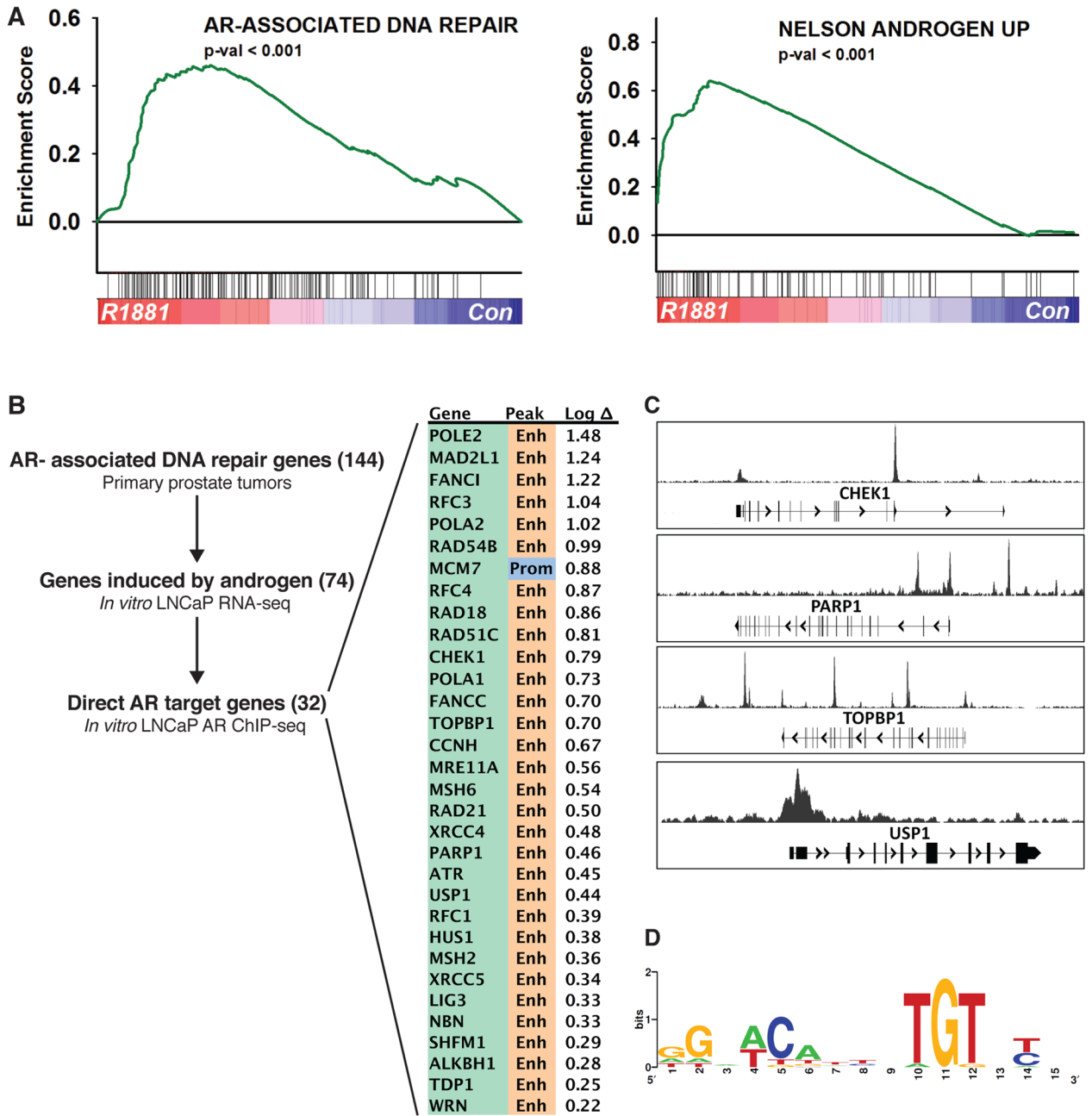


**Figure 2. A network of DNA repair genes are both induced by androgen and represent AR target genes**

**A.** Gene set enrichment analysis of LNCaP cell line grown in charcoal-stripped serum (CSS) in the presence of exogenous androgen (R1881), red, or control, blue. Previously defined AR-associated DNA repair signature enriched for in addition to other well-established AR signatures, such as Nelson *et al.* (20). **B.** Of the 144 gene AR-associated DNA repair signature, 72 genes are significantly induced by R1881 and of these genes 32 represent AR target genes by ChIP-seq. **C.** Examples of AR peaks on representative DNA repair genes. **D.** Motif analysis of the AR binding peaks of these 32 genes revealed the classic consensus AR-binding site.

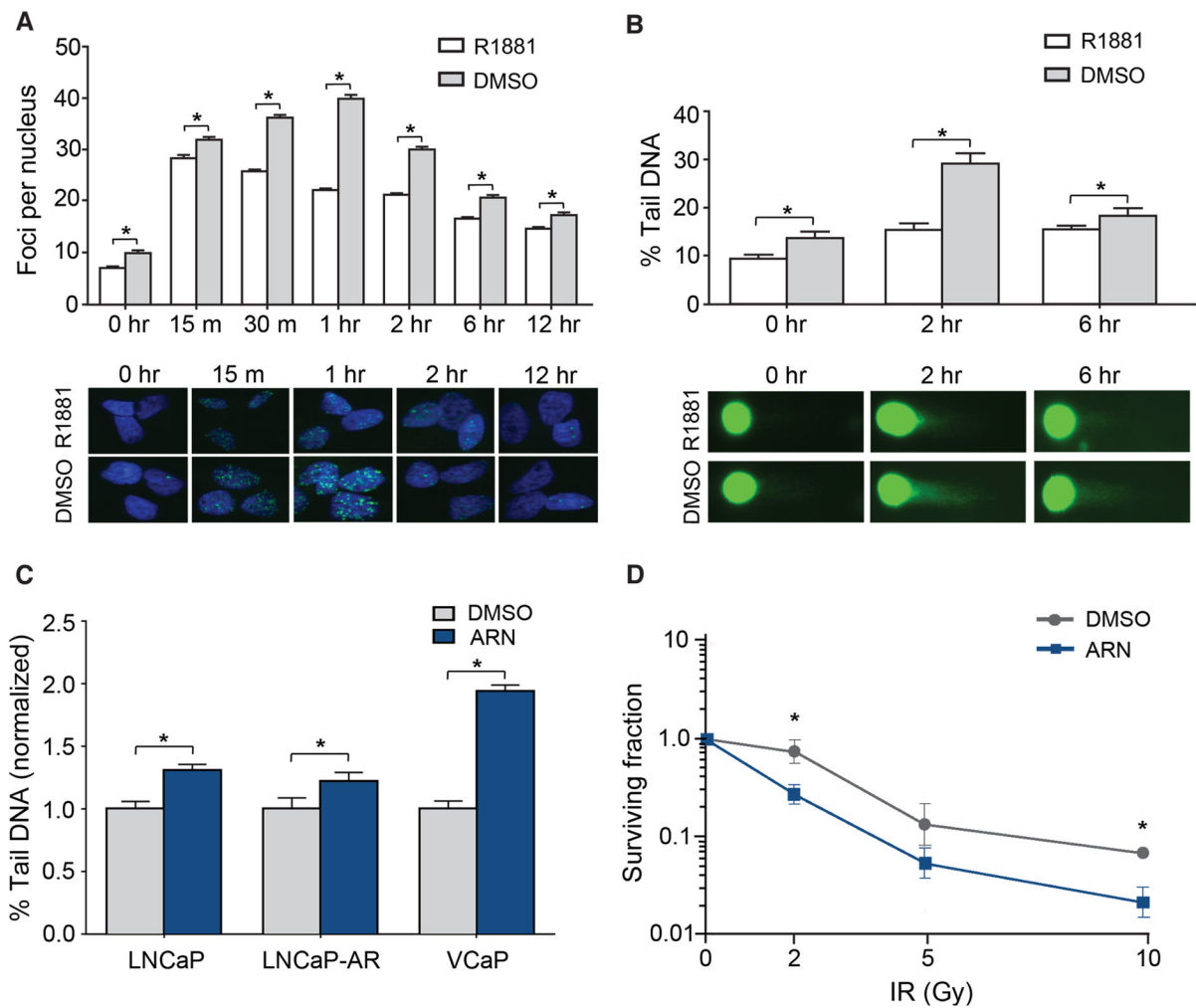


**Figure 3. Enhanced DNA repair in prostate cancer cells treated with androgen plus IR, decreased DNA repair and survival of cells treated with anti-androgen plus IR**

**A.** LNCaP cells, pretreated with either synthetic androgen (R1881) or mock, exposed to 2 Gy of IR, with DNA damage measured by gamma-H2AX foci. Under androgen-depleted conditions the foci peaked later and higher and resolved more slowly (\* =  $p < 0.001$ ). **B.** Neutral Comet assay of LNCaP cell line, showing increased double-strand breaks when cells irradiated under androgen-depleted conditions (\* =  $p < 0.001$ ). **C.** Neutral Comet assay of LNCaP, LNCaP-AR, and VCaP cells after 48 hours of treatment with second-generation anti-androgen (ARN-509) versus mock demonstrates increased double-strand breaks (\* =  $p < 0.001$ ). **D.** Clonogenic survival assay of LNCaP cells demonstrates decreased survival when irradiated in the presence of ARN-509 versus mock (\* =  $p = 0.02$ ).



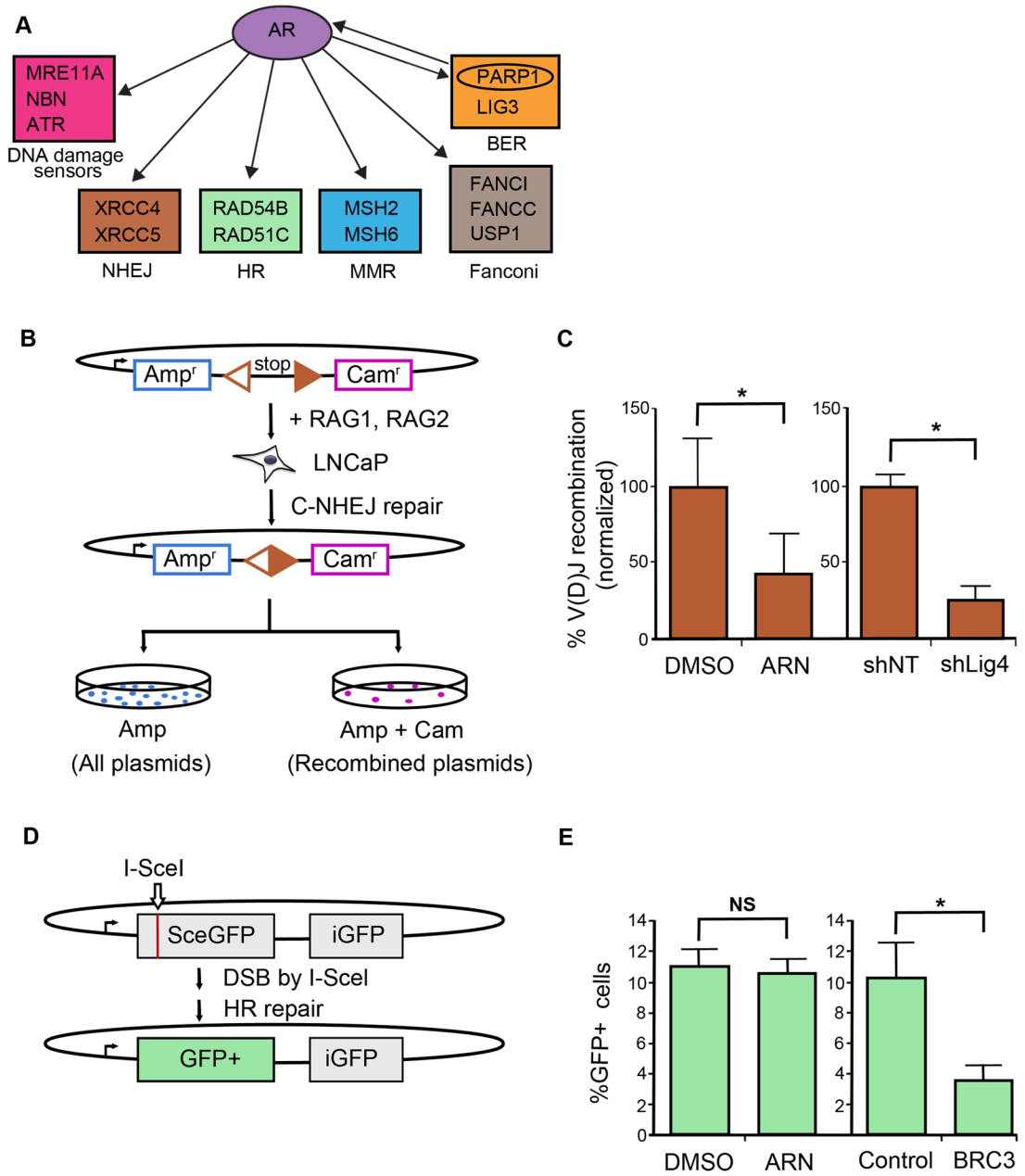


**Figure 4. AR regulates a network of DNA repair genes**

**A.** The AR-regulated transcriptome includes a number of DNA repair genes, one of which is the known AR-cofactor, PARP1. Other AR-regulated DNA repair genes play important roles in DNA damage sensing, non-homologous end joining (NHEJ), homologous recombination (HR), mismatch repair (MMR), and the Fanconi pathway. **B.** Schematic outlining the transient V(D)J recombination assay in which substrate along with RAG1 and RAG2 expression vectors are transfected into cells, after which bacteria are transformed with the rescued substrate and plated. Rescued substrate plasmids that fail to undergo recombination by classical NHEJ (C-NHEJ) only express the ampicillin (Amp) resistant gene, while those that successfully undergo recombination express both Amp and chloramphenicol (Cam) resistant genes. Recombination frequency can be calculated by the

ratio of colonies grown on the Amp + Cam plates compared to the Amp plates. **C.** Compared with control-treated LNCaP cells, treatment with ARN-509 significantly ( $p < 0.01$ ) decreases C-NHEJ as measured using transient V(D)J recombination assay. The magnitude of effect is comparable to that observed when Lig4, a known mediator of C-NHEJ, has been stably knocked down in a LNCaP cell line ( $p < 0.01$ ). **D.** Schematic outlining transient DR-GFP assay, in which DR-GFP contains direct repeats of two defective GFP genes with the upstream repeat containing a recognition site for the I-SceI endonuclease. When a double-strand break (DSB) is introduced by I-SceI followed by successful homologous recombination (HR) repair using the downstream copy as a template, it produces a functional *GFP* gene; GFP<sup>+</sup> cells are scored by flow cytometry. **E.** Compared with control-treated LNCaP cells, treatment with ARN-509 has no measurable effect upon HR repair as measured by the transient DR-GFP assay ( $p = 0.38$ ;  $n = 4$  transfections), while expression of the dominant negative BRC3 peptide ( $n = 3$ ) results in an approximately 2.8 fold reduction in HR compared to vector control ( $n = 2$ ) ( $p = 0.015$ ).